EGUN-ELBT reference trajectory correction in presence of ambient fields

Dobrin Kaltchev and Kyle Gao

May 10, 2014

Abstract

The effect of ambient magnetic field on the reference trajectory (orbit) in beam-line EGUN-ELBT is studied. We compute the deviation of central trajectory w.r.t. the vacuum chamber axis and find the required strength of *correctors or steering dipole magnets* to minimize this deviation. The final objective is to create an application tool written in either the *Mathematica* language or FORTRAN, which may be useful at commissioning.

1 Introduction

Considerations are presented on the effect of residual ambient fields in the EGUN-ELBT beam-line, a.k.a. ELBT – the E-linac injector extending from the gun cathode to the entrance in the first cavity. The reference design [1] (TRI-DN-10-08) assumes an ideal optics setup, focusing being provided by three short solenoids. In [1] the electron motion in solenoid fields is modeled with Astra, [2].

In this paper, for a beam line combining solenoid fields, ambient transverse (dipole) fields and correcting dipole magnets (steerers), we compute the reference orbit distortion before and after its correction. The level of ambient dipole fields for which no corrections would be needed is known to be very low – a fraction of a Gauss. The locations of the optics elements (solenoids and dipole correctors) are

placed as defined in [1], see Figure 1, while the ambient fields will be set to their measured levels [3] [1].

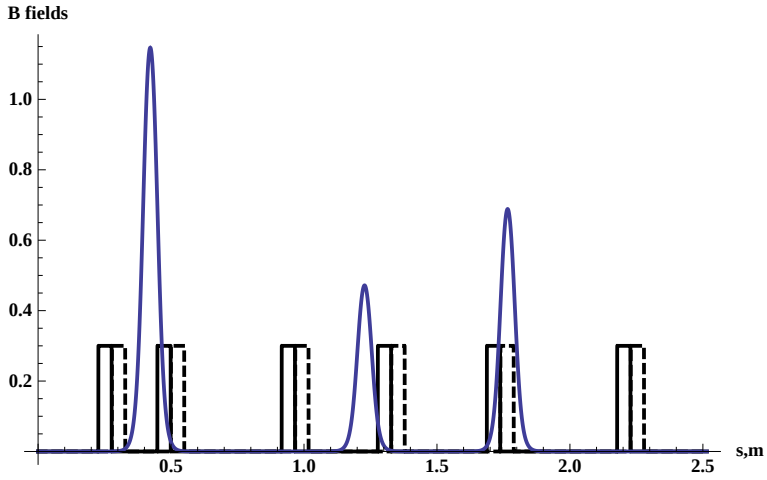

Figure 1: Locations of the optics elements in ELBT. Shown are the on-axis fields versus the coordinate s along the vacuum chamber axis: bell-shape for the solenoids taken at nominal strength ([1]), and tophat shape (rectangular with slightly rounded edges) for the corrector dipoles.

For the solenoids, the bell-shaped function describes the dependence of the longitudinal on-axis magnetic field on the coordinate s. It mimics the behavior of an iron-dominated solenoid. Once results from magnetic measurements have become available [3], the corresponding realistic shape was implemented in both our model and Astra. For the dipole correctors, focusing may be neglected, so when choosing the s-dependence of transverse on-axis magnetic field, our sole goal has been to assure agreement with the dipole optical element implemented in Astra. This implies: a tophat shape, rectangle with slightly rounded edges, and 2) horizontal and vertical correctors being artificially separated in longitudinal direction – solid and dashed lines on Fig. 1.

Consider the perturbed beamline: the case when some external ambient fields are present, but all dipole-corrector fields set to zero. The trajectory of the beam

[1] The effect of Helmholtz coil (decreasing) and cyclotron-field (increasing) on the ambient field is not included in this note.

centroid described by the reference-particle, the one that enters at $s = 0$ with kinetic energy 300 KeV and zero transverse coordinate and angle deviations, will deviate w.r.t. the chamber axis. This is referred to as the uncorrected reference trajectory (or orbit). The task is to find the settings for the 12 dipole correctors that minimize this deviation. Tracking the same reference particle as above now produces the corrected reference trajectory.

The organization of this paper is as follows.

Sect. 2 presents preliminary version of a web server that visualizes reference orbit, beam envelopes and bunch population by tracking with Astra. An XML format is used to describe of the EGUN-ELBT optics. The bump functions are passed to Astra in the form of numerical tables. Users can interactively execute Astra by choosing the entrance beam shape (assumed to be Gaussian).

Sect. 3 describes an optics code based on numerical solution of the equations of motion (EOM) for a single electron to find the reference orbit. The code exists in Mathematica and Fortran and, as this will be demonstrated, is in exact agreement with Astra. To provide a bridge to optics codes, the exact EOM are first linearized and then rewritten in Hamiltonian form (Appendix A).

Sect. 4 describes the method of optimization of dipole correctors. The mathematical treatment is based on the assumption that the ambient field is *known*. An interleaved correction scheme is applied with increased number of correctors involved.

In Sect. 5 we present our results on optimization of correctors for the section extending to cavity entrance. Three cases have been tried by varying the ambient-field region and imposed target: exact, i.e. zero orbit deviation everywhere, as opposed to zero only at monitors:

1. a single domain of ambient field located near the cathode with exact correction

2. measured ambient fields with an exact correction

3. measured ambient field with correction only at the three BPM's

Observations and conclusions are presented in Section 6.

2 Visualization of optics and beam on a web server

The ELBT optics described above and also basic characteristics of the electron beam may be visualized on a web server:

http://beam01.triumf.ca/optdata.

Following the decision of BD group made in 2013, the server was devised as a lattice storage tool, and should eventually provide:

- storage of E-linac sections (beam-optics lattices) in XML format;
- translation of the XML format to several of the optics codes used at Triumf: Astra, MadX, Dimad, Optim, Transoptr and COSY Infinity;
- basic optics calculation for a lattice by remotely executing an appropriate optics code through an Internet browser.

With regard to the ELBT, the above server allows to:

1. Display the HTML view of the optics up to the cavity exit. For example clicking on `Browse XMLs` and selecting `EGUN-ELBT` will result in what is shown on Figure 2.

2. Execute remotely the appropriate code. For example, click on the `Select Action` button and select `job "elbt-correctors"` will result in Astra run of beamline EGUN-ELBT with correctors (steerers) installed . What happens internally is that the XML source seen on Fig. 2 is automatically parsed into an

input deck and then `Astra` executed. All input and output files are stored in a working directory named `Work Dir`. Click on `Refresh` to check the job status. Typical execution time is about 10 seconds. A message "`all jobs done`" means that one can start browsing the working directory via `See Work Dir`. Some content of sub-directory `elbt-correctors` is shown on Figure 3.

3. Use `Modify Astra generator` to change the initial beam parameters, i.e. particle distribution at beam-line entrance. by editing the Astra input file `generator.in`. One can then repeat 2.

Figure 2 displays the XML format of optics including the cavity. and Figure 3 shows a 3D-geometry together with snapshots of the bunch at previously chosen markers defined in the XML script (these may be monitors). For illustration, the first corrector dipole is set at 0.5 Gs resulting in some displacement of the reference orbit (red line). The blue lines are the one-sigma r.m.s. envelopes in transverse (x and y) directions.

Figure 2: EGUN-ELBT in XML format. Here "at" refers to element center (it is the s-coordinate measured along beam path in mm starting from cathode face at $s = 0$).

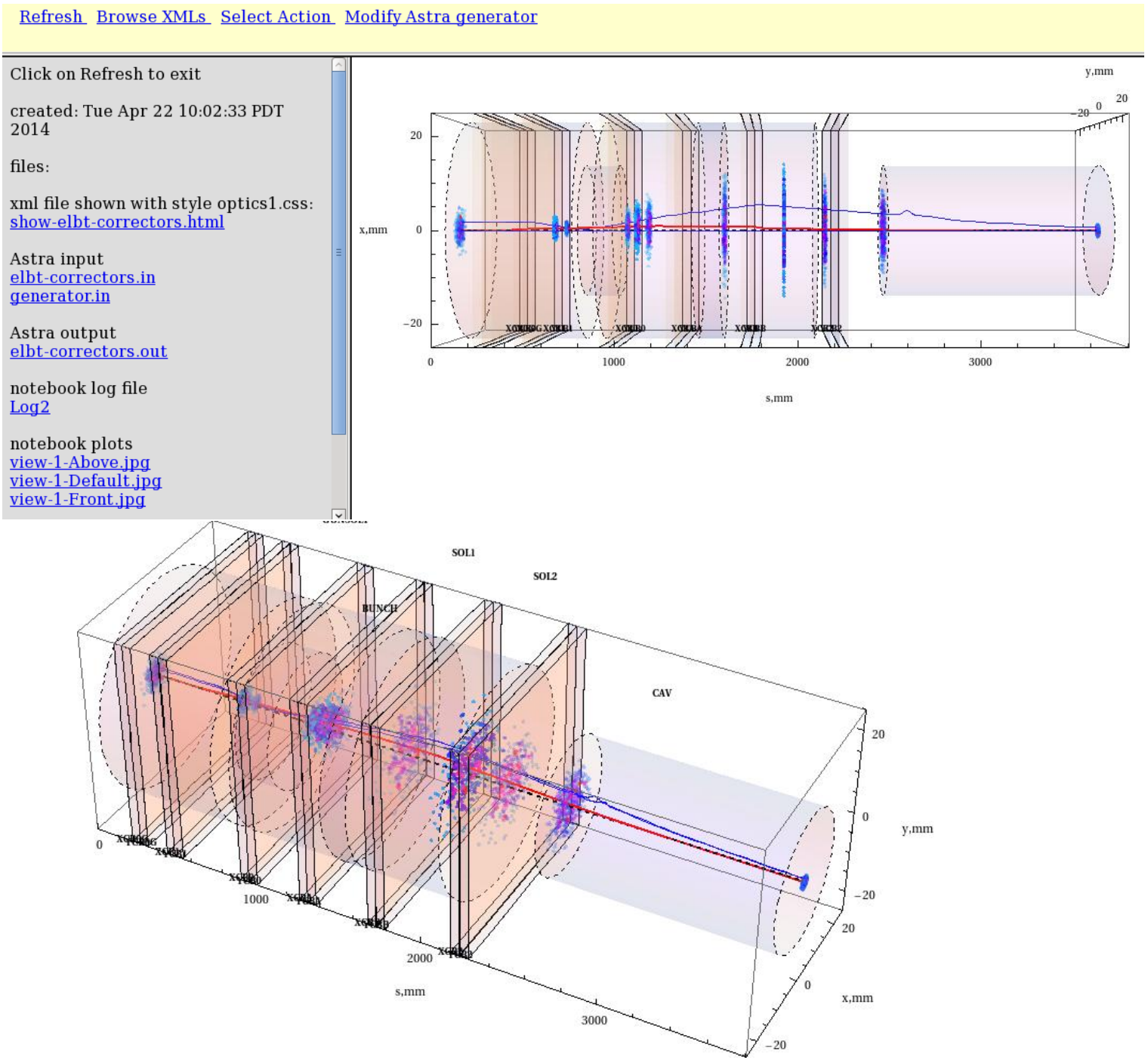

Figure 3: Top: Browser image of the working directory with ELBT geometry and beam (including the first cavity), view from above. Bottom: side view of ELBT and beam.

3 Tracking in combined Solenoid and Dipole fields

3.1 Equations of motion [6]

The equations describing the motion of an electron in combined, possibly overlapping, solenoid and dipole fields are given in Steffen, [6], in the laboratory frame, i.e. a fixed Cartesian coordinate system (x, s, y), where x is horizontal coordinate, y is vertical, and s is coordinate along the beam axis. These equations are:

$$\begin{array}{l} x' = v_x \\ {v_x}' = \frac{e}{p}\left(-B_y\left(1+{v_x}^2\right)+B_s v_y + B_x v_x v_y\right)\sqrt{1+{v_x}^2+{v_y}^2} \\ y' = v_y \\ {v_y}' = \frac{e}{p}\left(-B_s v_x - B_y v_x v_y + B_x\left(1+{v_y}^2\right)\right)\sqrt{1+{v_x}^2+{v_y}^2} \end{array} , \tag{1}$$

where $v_{x,y}$ denote derivatives in s: $v_x \equiv \frac{dx}{ds} \equiv x'$ and $v_y \equiv \frac{dy}{ds} \equiv y'$. The inverse rigidity is given by $\frac{e}{p} = \frac{1}{(B\rho)_{\rm beam}}$ with $(B\rho)_{beam} = 0.00210066$ T.m for 300 keV electrons.

The Eqns (1) have been encoded in *Mathematica* Version 7, or 8 [4]. Also a Fortran subroutines exist and can be downloaded here: `elbt.f`.

We substitute in (1) the *linearized* total magnetic field (solenoid and dipole) $\vec{B} = (B_x, B_s, B_y)$. Here B_s is the longitudinal field component of the solenoid $B^{\rm sol}(s)$ (with reversed sign) while $B_{x,y}$ are the transverse components each being the sum of a dipole contribution from the solenoid (through the derivative B_s') and of the dipole fields:

$$\begin{array}{rcl} B_x(s,x) &=& -\frac{1}{2}x\frac{dB_s}{ds}(s) + B_x^{\rm dip}(s), \\ B_s(s) &=& -B^{\rm sol}(s), \\ B_y(s,z) &=& -\frac{1}{2}y\frac{dB_s}{ds}(s) - B_y^{\rm dip}(s). \end{array} \tag{2}$$

As noted above, the dipole fields include ambient and corrector field

$$B_x^{\rm dip} = B_x^{\rm corr} + B_x^{\rm amb}$$
$$B_y^{\rm dip} = B_y^{\rm corr} + B_y^{\rm amb}.$$

Upon linearization the equations (1) become:

$$x'' - \frac{e}{p}B_s y' - \frac{1}{2}yB_s' - B_x^{\rm dip} = 0\ , \qquad (3)$$
$$y'' + \frac{e}{p}B_s x' + \frac{1}{2}xB_s' - B_y^{\rm dip} = 0\ .$$

The linear equations of motion in solenoid field (see [8], [10]) are obtained when substituting $B^{\rm xdip} = B^{\rm ydip} = 0$ and $S(s) = \frac{e}{p}B_s(s)$:

$$x'' - Sy' - \frac{1}{2}S'y = 0 \qquad (4)$$
$$y'' + Sx' + \frac{1}{2}S'x = 0\ .$$

The link from angles x', y' to canonical momenta p_x, p_y is given in Appendix A. It is shown how (4) can be derived from a second-order Hamiltonian in the beam frame.

For the on-axis magnetic field, a bell-function model is employed constructed from the function

$$B^{\rm sol}(s) = B_0\left[1 + \frac{(s-s_0)^2}{d^2}\right]^{-3/2}\ , \qquad (5)$$

with $B_0 = 755.446$ T and $d = 34.498$ mm. The shape (5) follows from the recent measurements of the field of the first solenoid [3], The accuracy of approximation is illustrated on Figure 4 (for $s_0 = 0$).

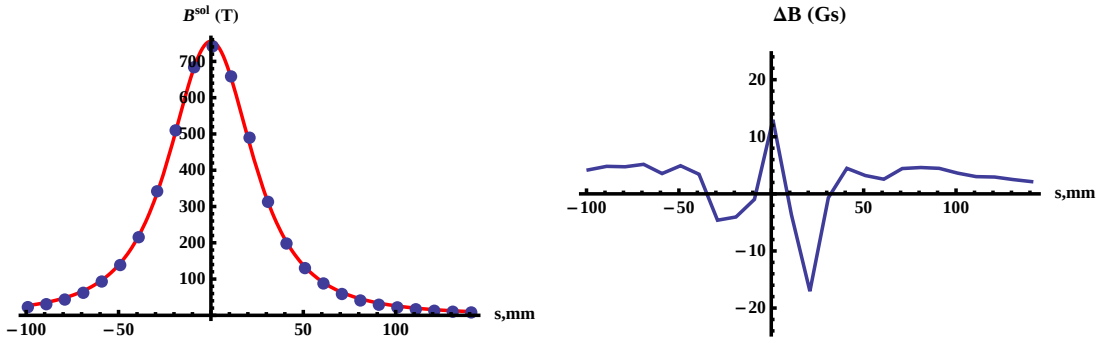

(a) Measured field according to [3] (blue dots) and the function $B^{\mathrm{sol}}(s)$ as in Eqn. (5) (red)

(b) Approximation error (red minus blue)

Figure 4: Measured solenoid fields, [3], and their approximation with the bell-shaped function Eqn. (5).

The steerer fields in x and y are described by steep tophat functions. When centered at $s = 0$:

$$B^{\mathrm{corr}}(s) = \frac{B_i}{2}\left[\tanh\frac{L_{\mathrm{eff}} - 2s}{2a} - \tanh\frac{L_{\mathrm{eff}} + 2s}{2a}\right] \tag{6}$$

with $L_{\mathrm{eff}} = 0.05$ m, $a = 0.0001$ m. B_i describes the strength of the i^{th} steerer in Tesla. This function, when shifted by s_i, approximately represents a field which is zero everywhere except for a distance of L_{eff} centered at s_i, where it takes the constant value of B_i.

3.2 Comparison with Astra

Figure 5 illustrates the agreement between the solution of Eqn (1) and the dipole optical element implemented in Astra. The first corrector dipole (red rectangle) is assigned a field $B^{\mathrm{xcorr}}(s)$ as described by (6) with B_1= 1 Gs (the deflection angle is 2.4 mrad). This is modeled in Astra as a hard-edge rectangular bend of length L_{eff}=5 cm.

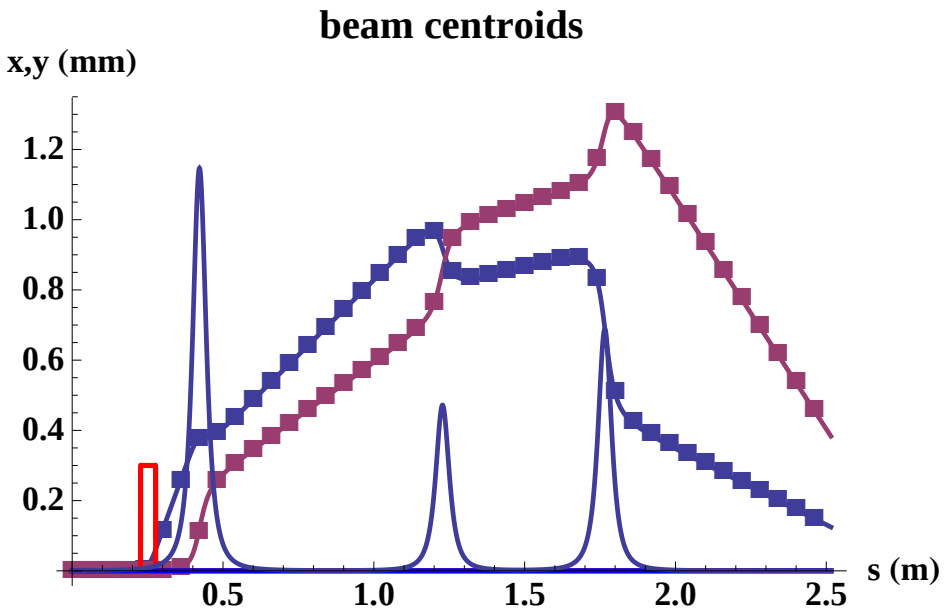

Figure 5: x- and y- projections of the beam centroid from cathode to cavity entrance as computed with *Mathematica* notebook that solves Eqns (1) with fields Eqn. (2) (solid lines) and Astra (filled rectangles). The optics element magnetic fields are also shown (arbitrary scale).

4 Reference orbit Correction

Ambient fields cause beams to deviate from reference orbit. This effect must be corrected by the beamline elements. For this purpose, only the dipole steerer fields (correctors) are varied while the solenoids are kept at their nominal settings. This correction is modeled using mathematical optimization methods described in this section.

4.1 General Algorithm

When correcting the orbit everywhere along the beamline, the correctors are divided evenly into groups of n correctors, according to the order they appear along the beamline, and correspondingly the beamline is divided into several s-intervals (sections). A section extends from the midpoint of the first corrector from its own

group to the midpoint of the first corrector from the next group. Starting from the location of the first dipole, the orbit is corrected section by section in a manner of "sliding correcting window".

The value of n i.e. the size of the window, is gradually increased to find compromise between best correction and and computing time. Notice that if n =12, all correctors are varied simultaneously to correct the orbit everywhere.

The above algorithm is easily modified for orbit correction strictly at the three BPM's.

4.2 Mathematica Implementation

A single electron, starting near reference orbit with initial conditions $(x, y, x', y') = (1\mu m, 1\mu m, 0, 0)$ at $s = 0$ is tracked. This particle experiences ambient fields and its motion deviates from reference orbit. The orbit is then corrected using "sliding correcting window". Within each group or section we apply interleaved correction scheme using Mathematica's numerical optimization methods. The Mathematica function `FindMinimum`, which locally minimizes a target function, was selected for this task [4]. A suitable target function for orbit correction will have corrector strengths as variables for which a minimum must exist. Furthermore that minimum must sufficiently optimize the orbit, that is, it must bring the generalized coordinates $\vec{x}(s) = (x, y, x', y')$ close to the generalized reference orbit (0,0,0,0) at requested locations along the longitudinal coordinate s.

The target function used is constructed by taking the absolute norm of the quadratic norm of the deviations at many locations s_i on the beamline.

$$\text{Target} = \sum_{i=1}^{N} (\sum_{j=1}^{4} w_j x_j^2(s_i))^{1/2} \tag{7}$$

Here x_j's are the components of (x, y, x', y'). The w_j's are weight factors taken to be 1 for angles. For positions, they are chosen to be 10 when minimizing

everywhere, and 3 when minimizing at BPM's only.

When correcting the orbit only at the 3 BPM's, then N=1 and `FindMinimum` is called once for each BPM by using correctors associated with it, and s_i is the location of the i^{th} BPM.

For corrections using groups of n correctors, the s_i's are defined as

$$s_i = s_0 + i\Delta S$$

$$\Delta S = \frac{s_{n+1} - s_0}{N}$$

where N is chosen to be 12, s_0 is the location of the first corrector in the group in longitudinal coordinate, and s_{n+1} is location of the first corrector in the next group (or $s = s_{\max} = 2.815$ m for the last corrector). In this scenario, `FindMinimum` is called for each group of correctors, minimizing the target function using only the correctors in the current group.

The 12 correctors are naturally grouped into 6 pairs. This naturally splits the beamline into 7 sections, 6 of which can be corrected (Figure 1). By choosing group size of two, the corrected s_i's matches the natural splitting of the beamline.

It was found that the target function does have a minimum which can be found by `FindMinimum` for reasonable initial conditions. Furthermore, the solution optimizes the orbit better than minimums of similar target functions using different weights or p-norms.

By choosing different powers in the target function, corrections can minimize absolute, quadratic, higher power mean, or maximum values. (Appendix B)

Furthermore, the correction is much faster when using smaller group size. Despite computing deviations at more coordinates, calling `FindMinimum` 12 times and optimizing correctors individually is faster by a factor of 20 when compared to optimizing the whole beamline calling `FindMinimum` once with all 12 correctors at the same. However, due to how s_i's are selected, different group size will result

in different corrected orbits. Figure 6 shows the radial deviation of the corrected orbit $R(s) = (x^2 + y^2)^{1/2}$ for different group sizes, color code and timing as in Table 1. The corrections are quite similar, except for group size of 1. It has trouble correcting angles due to uneven interval size while using group size 1, which causes the orbit to deviate after the last corrector.

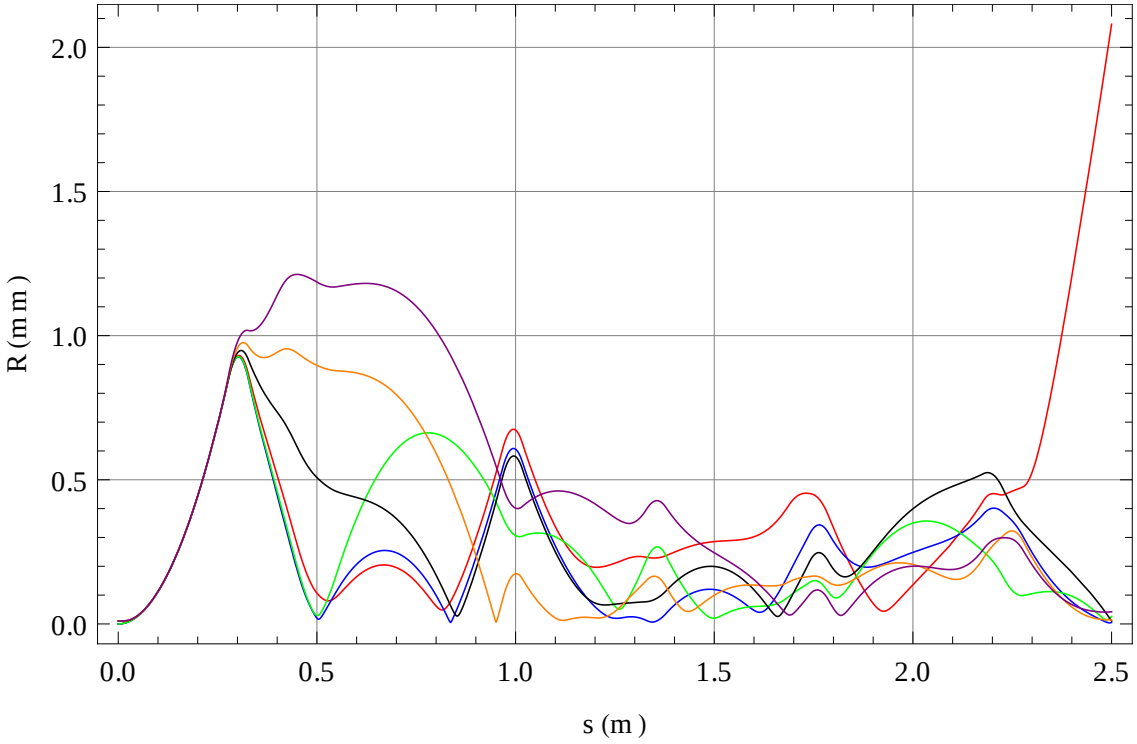

Figure 6: Corrected orbits for different group size,

Group size	color	run time (sec)
1	Red	49
2	Blue	321
3	Green	365
4	Black	373
6	Orange	430
12	Purple	1210

Table 1: Color codes and run times for Figure 6.

5 Results

5.1 Example of ambient field: 0.5 Gs near entrance

Figure 7 shows a sample calculation and also serves to illustrate our way of presenting the results. Here both reference trajectory (orbit) and fields are plotted on the same graph – red (or maroon) colors mean horizontal and blue vertical. A simple ambient field situated near the entrance (red dashed rectangle) is used, horizontal, i.e. deflecting in y direction, of constant value 0.5 Gs and covering length of 30 cm near the cathode. Shown are the resultant displacements in mm of the reference orbit projections in horizontal (x) and vertical (y) planes before (dashed) and after correction (solid). The corrector fields needed (dipole length =5 cm) are depicted in solid red (horizontal) and solid blue (vertical). The three solenoids are kept at nominal settings (bottom).

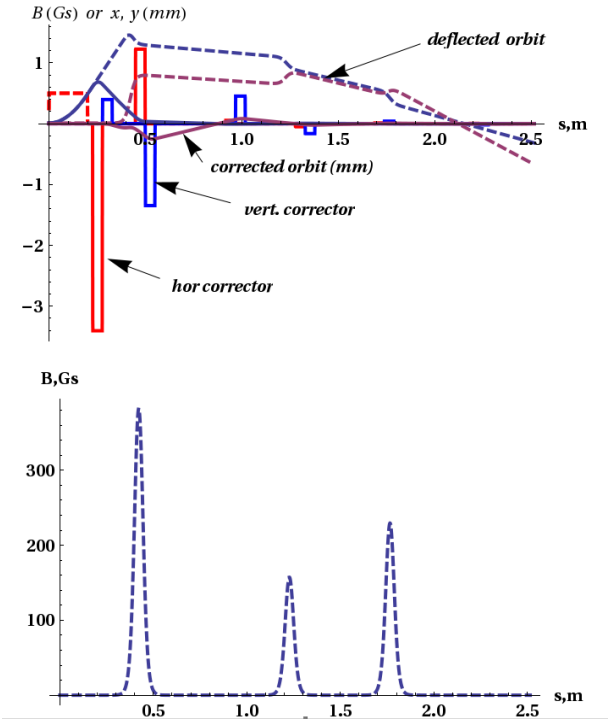

Figure 7: Top: A sample horizontal ambient field (red dashed rectangle) near the entrance, displacements (mm) of the design orbit and the corrector fields needed: red (vertical steerer) and blue (horizontal steerer). Bottom: solenoid fields (unchanged during correction).

5.2 Measured ambient field applied everywhere with correction requested everywhere.

Transverse ambient field is obtained from measurement along the beamline in intervals of 0.254 meters (10 inches) [2]. The data is then interpolated in Mathematica and the ambient field is added to the equations of motion. Figure 8 shows the resulting orbit and corrections. As shown in Figure 8, excellent solutions can be obtained from orbit corrections despite the overlapping of ambient field and corrector fields. Figure 9 shows an enlarged view of the solutions. The orbit deviates due to the ambient field but is repeatedly brought back by correctors. The positions and the angles are corrected along the beamline with the angles approaching 0 near the end.

[2] The data file is `20140220_cycOff_after250mHzDegauss.csv`

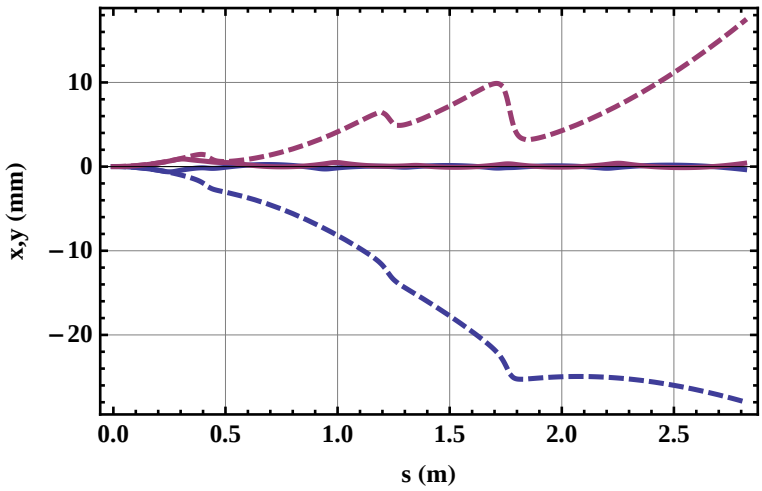

(a) Orbit before (dashed) and after (solid) correction.

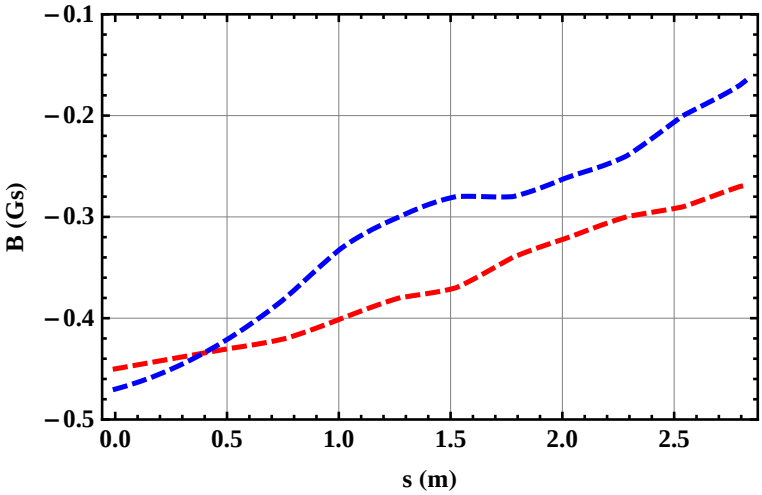

(b) Ambient field everywhere.

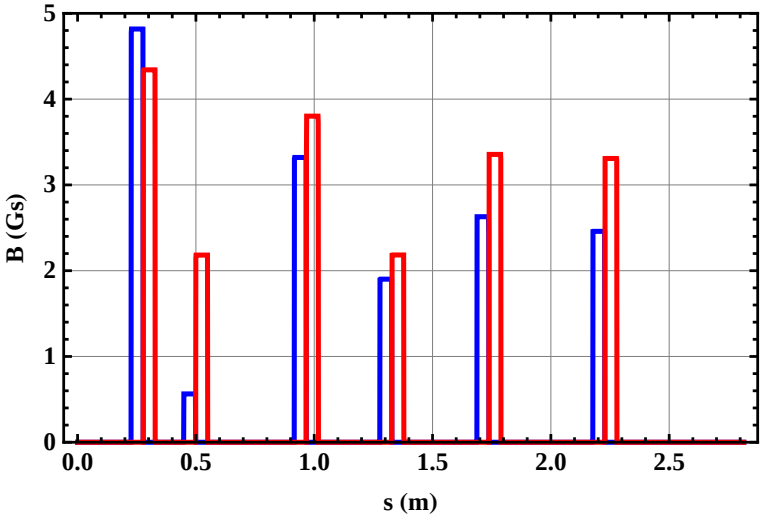

(c) Corrector fields (solid).

Figure 8: Measured ambient field applied everywhere and correction requested everywhere.

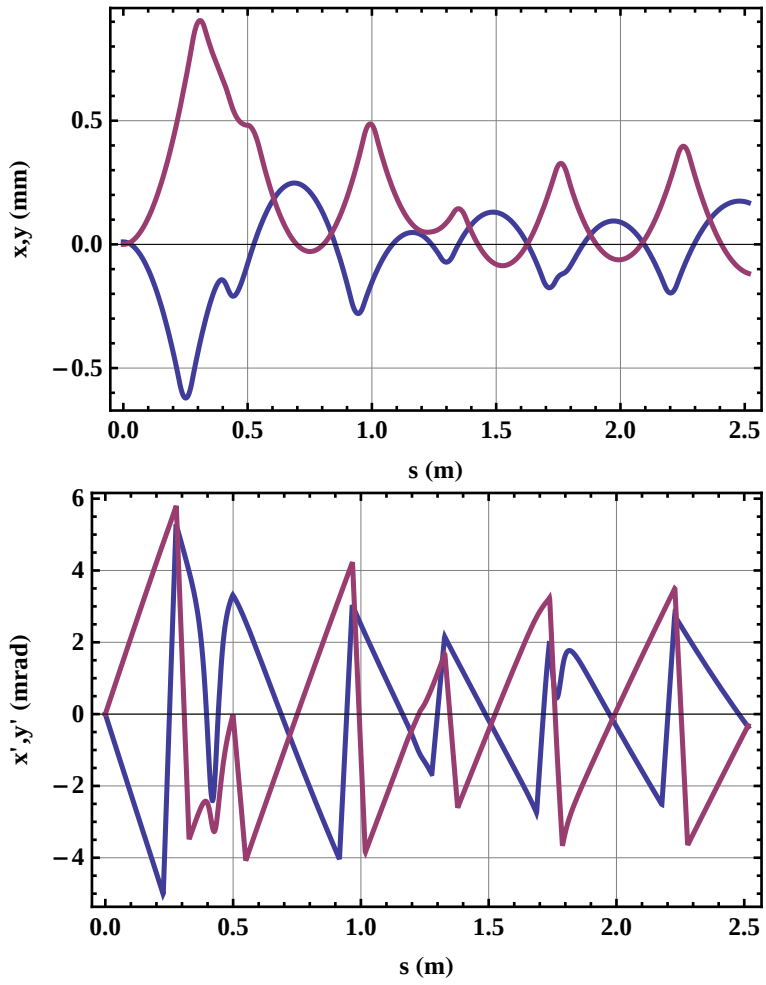

Figure 9: Corrected orbit: positions (x,y), same as on Figure 8 (a), and angles (x',y') along the beamline using group size of 2 and weight ratio =5 (5 times more weight on the coordinates than the angles).

5.3 Ambient field only in drifts with correction at the three BPMs

Assuming that correctors and solenoids act as shields against ambient field, a new ambient field is constructed to be zero inside correctors and solenoids, and take on measured values inside drifts. This requirement causes the ambient field is to appear piecewise continuous. However, it should be differentiable for the ease of solving the resulting equations of motion.

For this reason, the following ambient field was used:

$$\mathrm{Amb}(s) = \mathrm{AmbMeasured}(s)[1 - \sum_{i=1}^{N} B^{corr}(s - s_i)]. \tag{8}$$

The measured field is multiplied by 15 inverted steerer fields (6) of height 1, shifted up by 1. Each steerer field is centered at an s_i, the location of a corrector or solenoid. This new ambient field function satisfies our requirement and its equations of motion are solvable.

Figure 10 shows the new ambient field, the resulting orbit, and its correction at the 3 BPM's.

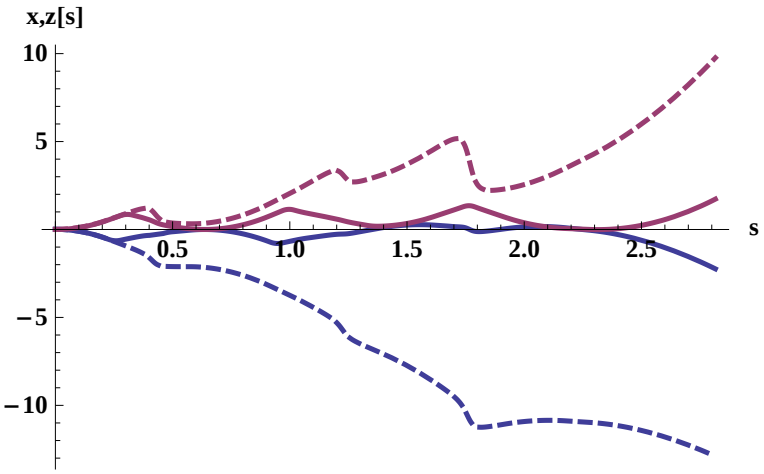

(a) Orbit before (dashed) and after (solid) correction.

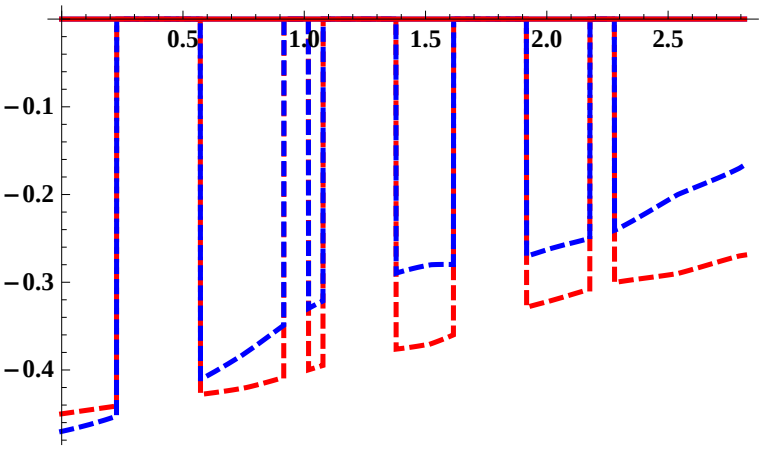

(b) Ambient field only in drift spaces.

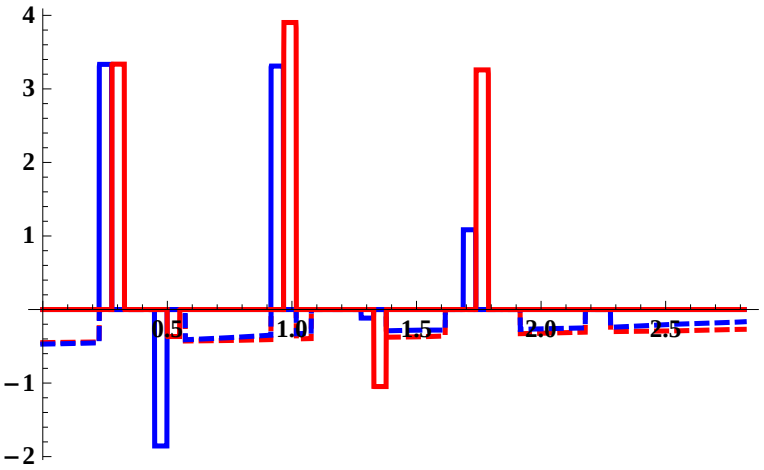

(c) Corrector fields (solid). Odd number correctors 1, 3 and 5 are much stronger that even ones.

Figure 10: Measured ambient field applied in drift spaces only and correction requested at the three BPM's.

BPM #	s,m	used correctors #	total correctors
1	0.63	1,2,3,4	2
2	1.12	5,6	1
3	2.17	7,8,9,10	2

Table 2: Correctors used to make Fig. 10 and 11. Shown is the BPM's position and the correctors used to correct orbit at this BPM.

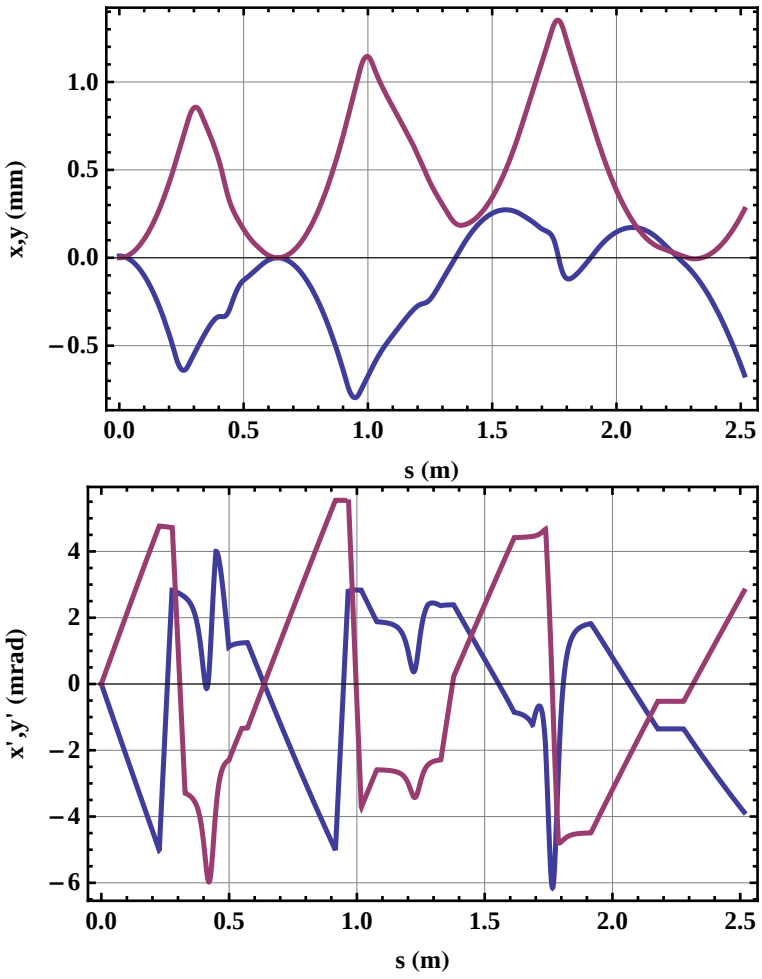

Figure 11: Corrected orbit : positions (x,y), same as Figure 10 (a), and angles (x',y') along the beamline using correctors as shown on Table 2 and weight ratio =5.

6 Summary and conclusions

We have used ambient field distribution that has a maximum of ~ 0.5 Gs in both planes located near entrance (Figure 8, middle). With this field the maximum uncorrected beam-centroid deviations was larger than 2 cm, assuming the field penetrates everywhere, and about half this value if the screening effect of the metal envelope in solenoids and steerers is taken into account.

1. In case of ideal correction (see Figure 8): a zero deviation requested everywhere (over dense set of locations), the corrected central trajectory was about 0.5 mm, all along the line except at the first kicker, which was also the strongest (6 mrad), and at the entrance of the first solenoid. The trajectory angles, or slopes. x' and y' at the cavity entrance can be matched to zero. Thus near the gun the ambient field could not be efficiently corrected. The corrector strengths are all about 3.5 - 5 Gs, except the second one, immediately after the first solenoid, which was about 2 Gs. The notebook used was `FindMin.nb`

2. In the closer to the reality case (see Figure 8): with included metal-envelope screening, but correcting only at the three BPMs, the maximum of corrected orbit is still about $\sim$ 1 mm, this time distributed uniformly along the line. Typical centroid deviations at cavity entrance were below 0.5 mm and angle 1-2 mrad. A clear corrector pattern is observed: only the odd-number 1st,3 and 5th correctors are found useful and stay at the same strengths as in 1) above, while the even-number ones are much smaller. The notebook used was `PieceWiseFindMinBPM.nb`.

...

Appendices

A Linear solenoid

The solenoid Hamiltonian, when expanded to second order: [3]

$$H = 1/2\left[(p_x + \frac{S}{2}y)^2 + (p_y - \frac{S}{2}x)^2\right] - \frac{p_\tau^2}{2} + \frac{p_\tau^2}{2\beta^2}\ . \tag{9}$$

By defining $S_2 \equiv \frac{S}{2}$, the equations of motion for the transverse coordinates are

$$\begin{aligned} x' &= p_x + S_2 y \\ p_x' &= (p_y - S_2 x)S_2 \\ y' &= p_y - S_2 x \\ p_y' &= -(p_x + S_2 y)S_2. \end{aligned} \tag{10}$$

We now show that (10) are equivalent to (4), see Baartman [9] and Guignard, [10]. First, we solve for p_x in the first equation of (10) and differentiate wrt s:

$$p_x' = x'' - S_2' y - S_2 y'.$$

Next, we substitute p_x' into equation 2 of (10)

$$x'' - S_2' y - S_2 y' = (p_y - S_2 x)S_2.$$

Using equation 3 of (10), this simplifies to:

$$x'' - S_2' y - S_2 y' = y' S_2. \tag{11}$$

This can be rearranged to become the first Eqn of (4). The second Eqn of (4) is derived in a similar manner. This proves that while the equations (10) contain no S' term, the y are equivalent to (4).

[3] The Hamiltonian from which (9) is derived can be found in Dragt [7], where (9) is denoted by K_2:

$$H = -\sqrt{1 + p_t^2 - (p_x - \tilde{A}_x)^2 - (p_y + \tilde{A}_y)^2 - \frac{2p_t}{\beta}} + \frac{1}{\beta^2} - \frac{p_t}{\beta}$$

This expression is to be expanded to second order with replaced $\tilde{A}_{x,y}$ by S.

The time dependent part is of no interest as it simply produces motion in a drift space (with $\tau = c(t - t_0)$):

$$\tau' = p_\tau(-1 + \frac{1}{\beta^2})$$
$$p'_\tau = 0\ . \tag{12}$$

Notice that $\tau' = \frac{p_\tau}{(\beta\gamma)^2}$ since $(-1 + 1/\beta^2) = \frac{1}{(\beta\gamma)^2}$.

B Appendix Target Function

Consider the p-norm of a vector, $\mathbf{X}$=$(x_1, ...x_n)$, defined for p $\geq$ 1.

$$|\mathbf{X}|_p = (\sum_{i=1}^{n} |x_i|^p)^{1/p}.$$

In general, a target function which must take into account the weighted contribution of deviation in canonical coordinates $\mathbf{X}$=$(x(s), y(s), p_x(s), p_y(s))$ at different position. This is done by taking a generalized mean of a generalized norm of $\mathbf{X}$ along the beamline.

Since only the locations and not the values of extrema in the target function are of interest, the function may be written using two p-norms:

$$(\sum_{i=1}^{N}(\sum_{j=1}^{4} w_j|x_j(s_i)|^b)^{a/b})^{1/a}.$$

However, the location of a local extrema of a positive target function is not shifted after raising the function to some exponent. This can be shown by considering an example target function T($\mathbf{X}$) positive everywhere, at a local minima T($\mathbf{X_0}$). It follows that T($\mathbf{X_0} + \delta\mathbf{X}$) $\geq$ T($\mathbf{X_0}$). Now consider taking every value of T in a small neighborhood around $\mathbf{X_0}$ and raising them to some positive real number p. Since T is always positive, we have:

$$T(\mathbf{X_0}) \leq T(\mathbf{X_0} + \delta\mathbf{X}) \iff T(\mathbf{X_0})^p \leq T(\mathbf{X_0} + \delta\mathbf{X})^p.$$

Furthermore, minimizing $|\mathbf{X}|_p$, will prioritize minimizing the absolute sum of individual x_i for smaller values of p. For large values of p, it will prioritize the minimizing the maximum value of $x_i's$. **http://mathworld.wolfram.com/Norm.html**

By adjusting w_j, a, b parameters of the previous formula, the target function whose minimum will best correct the orbit can found.

Figure 12 show that the $a = 1, b = 2$ make a better target function than other attempted values, these are the values we used for orbit correction. Furthermore, it can be seen that using a Maximum Value norm (Top: black curve, Figure 12) may cause issues due to the discontinuities of the resulting target function.

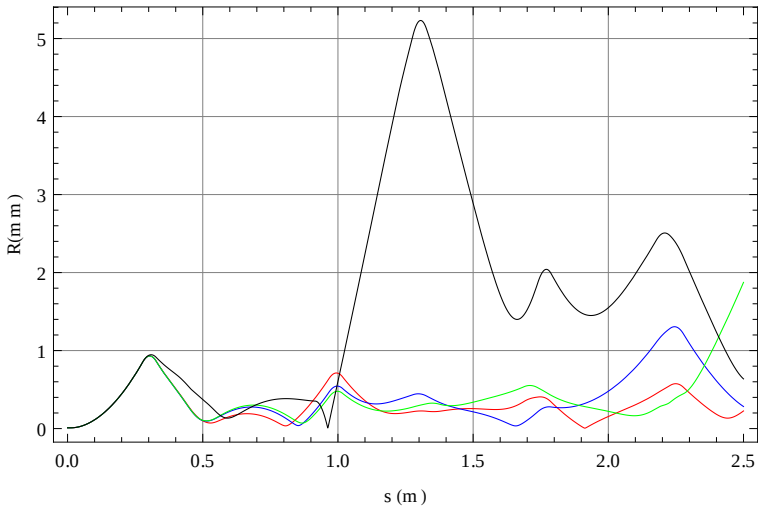

(a) a=1(red) 2(blue) 4(green) infinity(black), b is constant

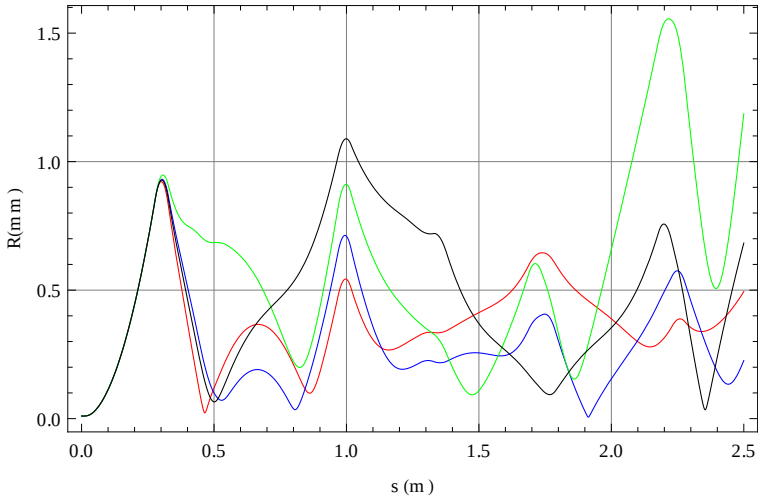

(b) b=1(red) 2(blue) 4(green) infinity(black), a is constant

Figure 12: Orbit distance R(s), after corrections for target functions using different a, b values.

References

[1] Y. Chao, E-Linac Major Components and Layout up to Exit of Injector Cryo-Module, Design Note TRI-DN-10-08, 17 Jan 2014.

[2] Klaus Flttmann, ASTRA, `http://www.desy.de/~mpyflo`

[3] T. Planche, private communication

[4] Wolfram Research, Inc., *Mathematica*, Version 7.0, Champaign, IL (2008).

[5] B. Champion, A. Strzebonski, Wolfram Mathematica Constrained Optimization

[6] , K. Steffen, Basic Course on Accelerator Optics, DESY, page 25 .

[7] A. J. Dragt, *"Numerical Third Order Transfer Map for Solenoid"*, NIM A298 (1990) 441-459

[8] G. Ripken, DESY 85-084, 1085

[9] R. Baartman, Talk at Snowmass, 2001.

[10] G. Guignard and J. Hagel, Hamiltonian treatment of betatron coupling, CERN report